

## R-Process Abundances and Chronometers in Metal-Poor Stars

John J. Cowan,<sup>1</sup> B. Pfeiffer,<sup>2</sup> K.-L. Kratz,<sup>2</sup> F.-K. Thielemann,<sup>3</sup> Christopher Sneden,<sup>4</sup> Scott Burles,<sup>5,6</sup> David Tytler,<sup>5</sup> and Timothy C. Beers<sup>7</sup>

cowan@mail.nhn.ou.edu, pfeiffer@vkcmzd.chemie.uni-mainz.de,  
klkratz@vkcmzd.chemie.uni-mainz.de, fkt@quasar.physik.unibas.ch,  
chris@verdi.as.utexas.edu, scott@rigoletto.uchicago.edu, tytler@ucsd.edu,  
beers@pa.msu.edu

Received \_\_\_\_\_; accepted \_\_\_\_\_

---

<sup>1</sup>Department of Physics and Astronomy, University of Oklahoma, Norman, OK 73019

<sup>2</sup>Institut für Kernchemie, Univ. Mainz, Fritz-Strassmann- Weg 2, D-55099 Mainz, Germany

<sup>3</sup>Department für Physik und Astronomie, Univ. Basel, Klingelbergstr. 82, CH-4056 Basel, Switzerland

<sup>4</sup> Department of Astronomy and McDonald Observatory, University of Texas, Austin, TX 78712

<sup>5</sup>Department of Physics and Center for Astrophysics and Space Sciences, University of California, San Diego, MS 0424, La Jolla, CA 92093-0424

<sup>6</sup>Department of Astronomy and Astrophysics, University of Chicago, Chicago, IL 60637

<sup>7</sup>Department of Physics and Astronomy, Michigan State University, E. Lansing, MI 48824

## ABSTRACT

Rapid neutron-capture (i.e.,  $r$ -process) nucleosynthesis calculations, employing internally consistent and physically realistic nuclear physics input (QRPA  $\beta$ -decay rates and the ETFSI-Q nuclear mass model), have been made. These theoretical computations assume the classical waiting-point approximation of  $(n,\gamma) \rightleftharpoons (\gamma,n)$  equilibrium. The calculations reproduce the solar isotopic abundances in detail, including the heaviest stable Pb and Bi isotopes. These calculations are then compared with ground-based and HST observations of neutron-capture elements in the metal-poor halo stars CS 22892–052, HD 115444, HD 122563 and HD 126238. The elemental abundances in all four metal-poor stars are consistent with the solar  $r$ -process elemental distribution for the elements  $Z \geq 56$ . These results strongly suggest, at least for those elements, that the relative elemental  $r$ -process abundances have not changed over the history of the Galaxy. This indicates that it is unlikely that the solar  $r$ -process abundances resulted from a random superposition of abundances from different  $r$ -process nucleosynthesis sites. This further suggests that there is one  $r$ -process site in the Galaxy, at least for elements  $Z \geq 56$ .

Employing the observed stellar abundances of stable elements, in conjunction with the solar  $r$ -process abundances to constrain the calculations, predictions for the zero decay-age abundances of the radioactive elements Th and U are made. We compare these (least-squares-fit ETFSI-Q) predictions with newly derived observational values in three very metal-poor halo stars: HD 115444, CS 22892–052 and HD 122563. Within the observational errors the observed ratio of [Th/Eu] is the same in both CS 22892–052 and HD 115444. Comparing with the theoretical ratio suggests an average age of these two very metal-poor stars to be approximately  $13.0 \pm \simeq 5$  Gyr, consistent with earlier radioactive age

estimates and recent globular and cosmological age estimates. Our upper limit on the uranium abundance in HD 115444 also implies a similar age. While there are still large uncertainties, the age estimate for both stars suggests radioactive age determinations may offer promise as an independent dating technique for the Galaxy, which specifically avoids uncertainties in Galactic chemical evolution models.

*Subject headings:* Galaxy: evolution — nuclear reactions, nucleosynthesis, abundances — stars: abundances — stars: individual (CS 22892–052, HD 115444, HD 122563, HD 126238) — stars: Population II

## 1. Introduction

Elemental abundances in metal-poor halo stars provide important clues to the chemical evolution of the early Galaxy. Since these stars are extremely old, their abundance patterns are living records of the first generations of Galactic nucleosynthesis. Much recent observational and theoretical work has concentrated on understanding the origin of neutron-capture elements in halo stars. These elements are those with atomic numbers  $Z > 30$  (or mass numbers  $A > 68$ ), thus comprising the majority of elements in the periodic table. Some isotopes of the neutron-capture elements may be built through neutron bombardment rates that are slow enough to allow all beta-decays to take place between successive neutron captures; this is called the *s*-process. Alternatively, short-duration rapid neutron bombardments that occur more rapidly than beta-decay rates can produce other neutron-capture element isotopes; this is the *r*-process. More generally, many isotopes may arise from a combination of both *s*- and *r*-processes, and disentangling the relative contributions of each of these to determine total elemental abundances has been difficult.

Many chemical composition studies of low-metallicity stars have detected the presence of a strong *r*-process component in the neutron capture element abundances (Spite & Spite 1978, Truran 1981, Sneden & Parthasarathy 1983, Sneden & Pilachowski 1985, Gilroy et al. 1988, Gratton & Sneden 1991, 1994; Sneden et al. 1994; McWilliam et al. 1995a, 1995b; Cowan et al. 1996, Sneden et al. 1996, Burris et al. 1998; McWilliam 1998). In addition, there has been increasing evidence suggesting a relative or scaled solar *r*-process abundance pattern in these stars, at least for the heaviest of these elements (Gilroy et al. 1988, Cowan et al. 1995, Sneden et al. 1996, Cowan et al. 1997).

Even though the elemental abundance patterns apparently are in agreement with a purely solar *r*-process distribution, these are necessarily sums over individual isotopic abundances. Frustratingly then, a solar *r*-process match to stellar elemental abundances

gives fewer constraints to their isotopic composition than would a direct observation of a solar isotopic  $r$ -process abundance pattern. In principle there exists a degeneracy in the sense that different non-solar isotopic abundance patterns might still fit a solar  $r$ -process elemental pattern. It is not impossible to produce identical abundances for approximately 30 elements with  $Z \geq 56$  through different mixtures of the approximately 80 individual isotopes of these elements. Goriely & Arnould (1997) have conducted such an exercise, showing that a series of several non-solar isotopic abundance distributions could produce a total elemental abundance pattern that might indeed match some of the neutron-capture elements in one low-metallicity star. However, this agreement cannot occur as a result of any random superposition of abundances. There has to be an intriguing conspiracy for compensation of the non-solar values of different isotopes in order to still fit a solar element composition. Thus, while the observation of a solar  $r$ -process elemental pattern is not an absolute proof for isotopic solar  $r$ -process abundances, it is nevertheless the most reasonable and probable conclusion.

This conclusion is further strengthened by the existence of a scaled solar  $r$ -process abundance pattern for many elements, not just in one low-metallicity star, but now in four stars (Snedden et al. 1996, 1998). The data for these stars are not restricted to a narrow region of elements (i.e., the rather flat inter-peak region near mass number 150), but now cover a wide elemental range from Ge ( $Z = 32$ ) through Pb ( $Z = 82$ ). These recently observed abundance patterns also agree with earlier findings, for a wide range of stars with varying metallicities, that the Ba/Eu ratio varies from a pure  $r$ -process ratio at low metallicities to a solar mix at solar metallicities (see McWilliam’s 1997 review and references therein; also McWilliam 1998, Burris et al. 1998). Magain (1995) recently attempted to estimate Ba isotopic abundances from synthetic/observed profile comparisons of a Ba II line in the very low-metallicity subgiant HD 140283. He concluded that a total solar system isotopic mix (i.e.,  $r$ - +  $s$ -process) provided the best match, implying a significant  $s$ -process

contribution to the neutron-capture elements in this star. However, François & Gacquer (1998) have repeated Magain’s investigation with superior spectroscopic data, and derive an isotopic mix for this same star that is consistent with a purely  $r$ -process synthesis origin.

There have been several difficulties, however, in determining the true nature of the stellar abundance pattern. First, most of the stellar abundances have been for the easily observed rare-earth elements, but these elements occur between the 2<sup>nd</sup> and 3<sup>rd</sup> neutron-capture peaks, i.e., in the relatively flat inter-peak region. The second  $r$ -process peak (near mass number,  $A$ ,  $\sim 130$ ) contains such elements as Te and Xe that at present have no identifiable solar and stellar transitions. The 3<sup>rd</sup> solar peak ( $A \sim 195$ , with elements Os, Ir and Pt) has mostly UV transitions and is thus not accessible to ground-based observations.

Additionally, there have been theoretical difficulties in predicting the neutron-capture element abundances. The first of these is the well-known uncertainty in the site of the  $r$ -process (see Cowan, Thielemann, & Truran 1991, Mathews, Bazan, & Cowan 1992, Meyer 1994 for further discussion of possible sites). Even promising scenarios, like the high entropy neutrino wind in supernovae (Takahashi, Witt, & Janka 1994, Woosley et al. 1994, Qian & Woosley 1996 ), have problems in obtaining the required entropies, and they have deficiencies in their abundance predictions (Freiburghaus et al. 1998). Thus, even though it would be preferred, it is currently not possible to provide results from a specific  $r$ -process site which give a good global fit to the observed, stable solar  $r$ -process abundances. Such fits have heretofore only compared stellar and scaled solar observed abundances. We need to develop tools to theoretically predict “equivalent” solar  $r$ -process for all neutron-capture elements, especially those of long-lived unstable nuclei (analogous to an infinite half-life, i.e., stable behavior).

A final problem is that the nuclei involved in the  $r$ -process are far from stability

and therefore the requisite nuclear data needed for reliable  $r$ -process predictions are not obtainable by experimental determination. However, there have been recent advances in theoretical prescriptions for very neutron-rich nuclear data (Möller et al. 1995, Aboussir et al. 1995, Möller, Nix, & Kratz 1997, Chen et al. 1995, Pearson, Nayak, Goriely 1996).

The detection of thorium in the ultra-metal-poor halo star CS 22892-052 (Snedden et al. 1994, Sneden et al. 1996, Cowan et al. 1997) in conjunction with the HST detections of the third  $r$ -process peak elements in some halo stars bears directly on nucleochronology. The long-lived radioactive nuclei (known as chronometers) in the uranium-thorium region are formed entirely in the  $r$ -process and can be used to determine the ages of stars and the Galaxy. In other low-metallicity stars the detection of neutron-capture elements in the (osmium-platinum) 3<sup>rd</sup>  $r$ -process peak, a nuclear region near that of uranium and thorium, confirms the full operation of the  $r$ -process for the synthesis of the heaviest ( $Z > 55$ )  $r$ -process elements during the early history of the Galaxy. The abundances of the stable elements in, and beyond, the 3<sup>rd</sup>  $r$ -process peak can then be used to help constrain the predictions of the initial (also known as production) values of the nuclei with  $A > 209$  and especially the long-lived radioactive chronometers, independent of knowing the site for the  $r$ -process.

The combination of the improved nuclear and stellar data will now allow more comprehensive and detailed attempts at a determination of the nature of the abundance patterns in these earliest Galactic stars. In this paper we analyze the production of the  $r$ -process elements in the solar system and in four metal-poor halo stars. In §2 we describe the  $r$ -process calculations and their relevance to the solar system isotopic abundance mix. Abundance comparisons between the calculations and the recent observations of four different metal-poor halo stars are made in §3. Age estimates for the Galaxy, based upon predicted and observed radioactive chronometers in the stars CS 22892–052 and HD 115444

are given in §4, and in §5 we conclude with a discussion of our results.

## 2. Calculations

We assume, as a working hypothesis, that the heavy element abundances of very low metallicity stars are given by a pure  $r$ -process composition. This assumption is supported by the observational evidence, at least for the elements beyond Ba, where data are available. We have analyzed  $r$ -process abundances with predictions from calculations in the waiting-point assumption (or  $(n,\gamma) \rightleftharpoons (\gamma,n)$  equilibrium) with a continuously improving nuclear data base (Kratz et al. 1988, Kratz et al. 1993, Thielemann et al. 1994, Chen et al. 1995, Pfeiffer et al. 1997). This approach is based on a continuous superposition of  $r$ -process components with a varying  $r$ -process path related to contour lines of neutron separation energies in the range of 4 to 2 MeV; the latter being determined by the combination of neutron number density and temperature. Such a procedure is also site-independent and essentially meant to provide a good fit to solar  $r$ -abundances, but it can also provide information regarding the type of conditions that a “real”  $r$ -process site has to fulfill. The fit is performed by adjusting the weight of the individual components for different neutron separation energies  $S_n(n_n, T)$  and the time duration  $\tau$  for which these (constant) conditions are experienced, starting with an initial abundance in the Fe-group. For a given (arbitrary) temperature,  $T$ ,  $S_n$  is a function of neutron number density,  $n_n$ , and the superposition weights  $\omega(n_n)$  and durations  $\tau(n_n)$  have a behavior similar to powers of  $n_n$ . This corresponds to a linear relation in  $\log(n_n)$  and is observed for a minimum of three components, when fitting the  $A=80$ , 130, and 195 abundance peaks (Kratz et al. 1993). This approach (although only a fit and not a realistic site calculation) also has the advantage that such a continuous dependence on physical conditions has embedded some relation to an (although unknown) astrophysical site. Therefore, one expects some predictive power also for mass regions that

are not explicitly fitted. This technique should be preferable to a multi-event superposition of components (Goriely & Arnould 1996) where the primary aim is to obtain a good fit by possibly even compensating for deficiencies in nuclear properties. Such an approach is not random but it changes randomly with different mass models. This superposition approach which employs thousand of components is equivalent to a high power polynomial fit to a specific mass interval, and thus one expects less predictive power outside that fit region.

Following our simplifying but physically predictive procedure, the best agreement with solar system  $r$ -process abundances was obtained when we employed the nuclear mass predictions from an extended Thomas Fermi model with quenched shell effects (i.e., ETFSI-Q) far from stability (Pearson, Nayak, & Goriely 1996) and the beta-decay properties from QRPA-calculations based on the methods described in Möller & Randrup (1990; see also Möller et al. 1997), while making use of the beta-decay Q-values of the afore-mentioned mass model.<sup>8</sup> For  $T_9 = 1.35$  this led to superpositions of the form  $\omega(n_n) = 1.494 \times 10^7 n_n^{-0.3408}$  and  $\tau(n_n) = 6.97 \times 10^{-2} n_n^{0.062}$  sec. The  $(n, \gamma) \rightleftharpoons (\gamma, n)$  equilibria on which the  $r$ -process calculations are based, will likely be obtained in any astrophysical environment with conditions in excess of  $n_n = 10^{20} \text{ cm}^{-3}$  and  $T = 10^9 \text{ K}$ , as expected from all possible sites (Meyer 1994). The major remaining question is due to possible effects of the freeze-out in realistic astrophysical sites when neutron density and temperature decline below the above mentioned limits. Thielemann et al. (1998) and Freiburghaus et al. (1998) could show with full network calculations, and without the assumption of equilibria, that these freeze-out effects are small, when mass models which include shell quenching far

---

<sup>8</sup> The choice of this mass formula is strengthened by recent experimental results (Kratz 1998) for very neutron-rich Cd isotopes. Comparison of masses deduced in these experiments are in better agreement with the ETFSI-Q predictions in this mass regime than with any other commonly used mass formula.

from stability are used. They also showed that the smooth superposition of results from different neutron separation energies with declining weights for smaller  $S_n$ -values can be translated into an almost constant entropy superposition of full network calculations for masses with  $A > 110$ . The coefficients and powers were obtained from a least square fit to solar  $r$ -abundances with the nuclear input discussed above.

We have used this physically motivated fitting procedure, which apparently reproduces the stable solar  $r$ -process abundances very well with a simple and robust superposition scheme, for the calculations in this paper. Here we have also extrapolated the calculations into unknown territory, specifically the actinides. Early applications of this scheme were only applied to fit abundances up to the  $A = 195$  peak, where individual isotopic data are available. The challenge is to find some features which provide a measure of the accuracy for all nuclei with masses  $A > 195$ , including the unstable actinides in alpha decay chains (Thielemann et al. 1994). In fact, there exist some observational constraints for these mass regions as well. Up to  $A = 205$ , isotopic abundances stemming from the beta-decay of  $r$ -process progenitor nuclei (as in the lighter mass regions) are available for a fit. The abundances of the  $^{206,207,208}\text{Pb}$  isotopes and  $^{209}\text{Bi}$  also contain additional information and are dominated by contributions from alpha-decay chains of isotopes with  $A > 209$ <sup>9</sup>. In Figure 1 we show the results of our calculations, before (dashed line) and after considering beta-decay and alpha-decay chains with short half-lives (solid line). As demonstrated earlier by Pfeiffer et al. (1997), this theoretical prescription described above provides excellent agreement with the observed solar abundances (small filled circles in Figure 1) for  $A > 195$ .

---

<sup>9</sup>For  $^{206}$  and  $^{207}\text{Pb}$ , for example,  $\beta$ -decay from the  $r$ -progenitors back to these isotopes amounts to only 5%, whereas 95% of the solar abundance values come from alpha back-decays of trans-lead isotopes. Similarly, for  $^{209}\text{Bi}$  the  $\beta$  contribution is about 7%; but for  $^{208}\text{Pb}$  the  $\beta$ -decay contribution amounts to roughly 15%.

Experiments have demonstrated that there is a large  $r$ -contribution to the Pb A=208 and 209 isotopes (Käppeler et al. 1989, Käppeler 1998). The fact that we can reproduce the solar Pb  $r$ -abundances, produced mainly from alpha back-decay from the heavy mass region beyond A = 209 up to about 250, where (apart from Th and U) no “observables” exist to tune our fits, gives us confidence that we are correctly predicting the radioactive actinide abundance values as well.

Our results demonstrate that all possible observables related to actinide abundances are satisfied, in fact, with an extension of the same power laws for  $\omega$  and  $\tau$  components up to  $n_n$  of  $3 \times 10^{27}$ . (A further extension to higher neutron densities has no effect, as the weights become so small that such components do not contribute.) This has the advantage that no additional parameter (like an upper limit for  $n_n$  components) is required. The remaining abundances of  $^{232}\text{Th}$  ( $\tau_{1/2}=1.405 \times 10^{10}\text{y}$ ),  $^{235}\text{U}$  ( $\tau_{1/2}=7.038 \times 10^8\text{y}$ ) and  $^{238}\text{U}$  ( $\tau_{1/2}=4.468 \times 10^9\text{y}$ ) will then, after their production, decay on their long decay-times.

Fission during the  $r$ -process was neglected in the calculations, because experimental data Hoff (1986,1987) and theoretical investigations (Cowan et al. 1987; Cowan, Thielemann, & Truran 1991) have shown that to first order fission is unimportant. After the end of the  $r$ -process we assumed spontaneous fission for nuclei beyond A = 257 (i.e.,  $^{257}\text{Fm}$ ). These nuclei will make no contribution to nuclei in mass range A=232-256 (which includes the Th and U isotopes), and so we included only “lighter” nuclei in the decay chains. Further, the abundances of nuclei with A>195 are predicted well by our model, including a correct prediction for the  $r$ -process contribution to the A=208,209 nuclei. These nuclear abundances are produced by alpha-decay chains starting in the mass region A=232-256. This gives a strong indication that the total amount of matter in the A=232-256 mass range is well predicted within this model. While extrapolations always involve some risk, the pleasing agreement noted here suggests that our calculations also have good predictive

power in this region of the nuclear chart.

To summarize this section, the excellent fit of our calculations to the solar system isotopic abundance distribution for  $A > 130$  suggests that one type of astrophysical event has been responsible for  $r$ -process production throughout this mass range. We cannot yet identify what type of event that was, but we expect that the conditions that created the processed matter to have varied smoothly. We caution the reader that our insufficient knowledge of the properties of nuclei far from stability could contribute to uncertainties in the abundance predictions for the chronometer elements Th and U. We address this issue in more detail in §4.

### 3. Abundance Comparisons

We next compare our theoretical  $r$ -process calculations with solar system  $r$ -process and stellar elemental abundance distributions. In Figure 2 we consider abundance data for the ultra-metal-poor star CS 22892-052 ( $[\text{Fe}/\text{H}] \simeq -3.1$ ).<sup>10</sup> The observations from Sneden et al. 1996 are indicated by large filled squares, while the small squares are the solar system  $r$ -process abundances connected by a dashed line. The solar elemental abundances are of course sums over the isotopic abundances, and these are based on deconvolving the total solar system abundances (Anders & Ebihara 1982, Anders & Grevesse 1989) into  $s$ - and  $r$ -process abundance fractions using the neutron capture cross sections of Käppeler et al. (1989) and Wisshak et al. (1996; see also Sneden et al. 1996 and Burris et al. 1998 for details). The solid line in Figure 2 indicates the predicted abundances from the ETFSI-Q

---

<sup>10</sup>We adopt the usual spectroscopic notations that  $[A/B] \equiv \log_{10}(N_A/N_B)_{\text{star}} - \log_{10}(N_A/N_B)_{\odot}$ , and that  $\log \epsilon(A) \equiv \log_{10}(N_A/N_H) + 12.0$ , for elements A and B. Also, metallicity will be arbitrarily defined here to be equivalent to the stellar  $[\text{Fe}/\text{H}]$  value.

least-square-fit calculations. Both the solar data and the predicted  $r$ -process abundances have been scaled vertically downward to account for the much lower metallicity of this star with respect to the sun. It is clear from the figure that the stellar data, the scaled solar abundances and the theoretical  $r$ -process abundances are coincident, at least for the stable elements Ba ( $Z = 56$ ) and above.

Figure 3 shows abundances for the very metal-poor ( $[\text{Fe}/\text{H}] = -2.7$ ) halo giant HD 115444. It includes the ground-based data (an average of the observational values from Griffin et al. 1982 and Gilroy et al. 1988; see also Sneden et al. 1998) indicated by open squares, while HST data from Sneden et al. (1998) are indicated by solid squares. In this figure we also include a new abundance value for thorium and an upper limit (as an arrow) on uranium. These radioactive elements will be discussed in §4. While Os was detected with somewhat large error bars in CS 22892-052, there is much more extensive 3rd  $r$ -process peak data available for HD 115444 (due to the HST observations). Sneden et al. (1998) have shown the similarity between the solar system  $r$ -process elemental curve and the data (both ground-based and space-based) all the way through the 3rd  $r$ -process peak for this star. Our new  $r$ -process theoretical calculations (the solid line in the figure) further confirm this result.

Figure 4 illustrates abundances for HD 122563, a star of approximately the same metallicity as HD 115444. However, HD 122563 is much less abundant in neutron-capture elements than is HD 115444, and only upper limits (indicated by arrows) for the 3rd  $r$ -process peak elements were obtained by Sneden et al. (1998). The ground-based data are averages of a number of studies (as discussed in Sneden et al. 1998). Both the solar system scaled  $r$ -process curve and our new  $r$ -process calculations are consistent with the available ground-based data and the upper limits for HD 122563 for elements with  $Z \geq 56$ .

The fourth halo star for which there is extensive data is HD 126238. This star with a

metallicity of  $[\text{Fe}/\text{H}] = -1.7$  is more metal-rich than the previously discussed stars. Cowan et al. (1996) and Sneden et al. (1998) have reported HST detections of the 3rd  $r$ -process peak elements along with Pb in this star, and those data are plotted in Figure 5. We again see the similarity in the abundance pattern for the heaviest neutron-capture elements in this star and the scaled solar  $r$ -process abundances, both predicted by our calculations and by actual solar data. There is, however, some deviation between the Ba abundance (a predominantly  $s$ -process element) and the  $r$ -process curves, which may indicate the onset of Galactic  $s$ -processing already at this higher metallicity (see also Cowan et al. 1996, Sneden et al. 1998). It is possible that some  $s$ -processing might have contributed also to the Pb abundance, although our data are not adequate to show such an enhancement.

The overall  $r$ -process to Fe ratio at low metallicities is highly variable. This was first noted by Gilroy et al. (1988), and is certainly evident in the four stars considered here. Specifically, the  $[\text{Eu}/\text{Fe}]$  ratio is +1.56 in CS 22892–052 (Sneden et al. 1994), +0.70 in HD 115444 as found in this paper, –0.44 in HD 122563 (Gratton & Sneden 1994) and +0.17 in HD 126238 (Gratton & Sneden 1994). Burris et al. (1998) will discuss this phenomenon more extensively. These results demonstrate that individual  $r$ -process events are resolved, on time scales probably shorter than Galactic mixing time-scales, but that the  $r$ -process abundances in each event are apparently well reproduced by a solar  $r$ -composition.

#### 4. Chronometers

Actinide chronometers have been used to determine Galactic ages by (i) predicting  $^{232}\text{Th}/^{238}\text{U}$  and  $^{235}\text{U}/^{238}\text{U}$  ratios in  $r$ -process calculations, (ii) applying them in Galactic evolution models, which include assumptions about the histories of star formation rates and  $r$ -process production, and finally (iii) comparing these ratios with meteoritic data, which provide the Th/U and U/U ratios at the formation of the solar system. Low-metallicity

stars have the advantage that one can avoid uncertainties introduced by chemical evolution modeling. The metallicities of the halo stars for which neutron-capture element data have become available range from  $[\text{Fe}/\text{H}] = -3$  to about  $-2$ . Typical evolution calculations suggest roughly that  $[\text{Fe}/\text{H}] = -1$  ( $10^9\text{y}$ ),  $-2$  ( $10^8\text{y}$ ),  $-3$  ( $10^7\text{y}$ ). Even if this estimate is uncertain by factors of 2-3, very low metallicity stars most certainly were born when the Galaxy was only  $10^7 - 10^8\text{y}$  old, a tiny fraction of the present age of the Galaxy. Thus the neutron-capture elements observed in very low metallicity stars were generated in one or at most a few prior nucleosynthesis episodes. These events had to have occurred on timescales very short in comparison to thorium decay ages. Thus, no error is made by simply adding these contributions, without considering decays, and treating them as one abundance distribution which undergoes decay until the present time. Any prior Galactic evolution can therefore be treated as a single  $r$ -process event incorporated into the observed star.

#### 4.1. New Observations

Snedden et al. (1996) used the technique described above in deriving a thorium-based age for CS 22892-052. But one star's age can hardly be assumed to stand for the whole low metallicity end of the galactic halo; detailed analyses must be done for other stars with high neutron-capture element abundance levels. An obvious candidate is HD 115444. It is about 0.3 dex more metal-rich than CS 22892-052, and has more moderate overabundances of neutron-capture elements (e.g.,  $[\text{Eu}/\text{Fe}] \simeq +0.7$ ). However, it is an easier star for detailed spectroscopy, as it is much the brighter star ( $V = 9.0$  against 13.1 for CS 22892-052). Therefore new ground-based UV and blue spectra of HD 115444 having high resolution ( $R \simeq 50,000$  to  $60,000$ ) and high S/N ( $\simeq 75$  to  $200$  near  $\lambda 4000 \text{ \AA}$ ) have been gathered with the McDonald Observatory 2.7m telescope and 2D-coudé spectrograph (Tull et al. 1995) and the Keck I HIRES (Vogt et al. 1992). An extensive analysis of this star is

in preparation (Eriksson et al. 1998); here we discuss preliminary analysis of only the chronometer elements.

In Figure 6 we show small spectral regions surrounding two Th II lines and one U II line in our data. The observed spectra are co-added data from the Keck and McDonald raw spectra; significant noise reductions in the spectra were achieved by the averaging of the spectra. Superimposed on each observed spectrum are four synthetic spectra in which only the abundance of thorium or uranium has been allowed to vary. To compute these synthetic spectra, we employed the current version of the line analysis code of Sneden (1973). We adopted the model atmosphere for HD 115444 derived by Pilachowski et al. (1996); the atomic/molecular line lists for each spectral region are described briefly below.

The Th II line at  $\lambda 4019.13 \text{ \AA}$  in HD 115444 is easily seen in the observed spectrum displayed in the top panel of Figure 6. The contaminating absorptions to this complex feature are also apparent. We used the line list described in Sneden et al. (1996), which was based on earlier studies of François et al. 1993 and Morell et al. 1992), but here we added two  $^{13}\text{CH}$  lines to the list. Norris, Ryan, & Beers (1997) have demonstrated that there are possibly severe blending complications to the Th II feature caused by these  $^{13}\text{CH}$  lines (see their Figure 1). The  $^{13}\text{CH}$  contamination is greatest in those halo giants with either strong CH bands and/or low  $^{12}\text{C}/^{13}\text{C}$  ratios. From analysis of  $^{12}\text{CH}$  and  $^{13}\text{CH}$  lines in other spectral regions, we estimate  $^{12}\text{C}/^{13}\text{C} \simeq 7\text{--}8$  for HD 115444. The overall CH band strength was a free parameter that was adjusted to match the  $^{13}\text{CH}$  doublet at  $\lambda\lambda 4020.0, 4020.2 \text{ \AA}$ , and then the  $^{13}\text{CH}$  absorption at  $\lambda 4019 \text{ \AA}$  was determined by this band strength, the transition probability ratio between the relevant  $^{12}\text{CH}$  and  $^{13}\text{CH}$  lines, and the  $^{12}\text{C}/^{13}\text{C}$  ratio. The major remaining contamination of the Th II feature is due to Co I (chiefly at  $\lambda 4019.3 \text{ \AA}$ ); and we altered the assumed Co abundance to match this absorption. Finally, we call attention to the partial Nd II blend at  $\lambda 4018.84 \text{ \AA}$ ; its strength in our HD 115444

spectrum is well matched by the Nd abundance recommended in earlier analyses of this star (Griffin et al. 1982, Gilroy et al. 1988). With these features accounted for, the remaining absorption near  $\lambda 4019 \text{ \AA}$  is attributed to Th II, and we deduced  $\log \epsilon(\text{Th}) = -2.10 \pm 0.1$ , the uncertainty being a combination of goodness-of-fit, continuum placement, and blending agent uncertainties.

Having a such good resolution and low noise spectrum of this star, we conducted a search for other strong Th II transitions. This exercise proved mostly fruitless, yielding only a possible line at  $\lambda 4086.52 \text{ \AA}$  that is more than 4 times weaker than the  $\lambda 4019 \text{ \AA}$  line. The observed spectrum given in the middle panel of Figure 6 shows no obvious Th II absorption. Nevertheless, we constructed a line list for features near the  $\lambda 4086 \text{ \AA}$  line from Kurucz’s extensive atomic and molecular line lists (see Kurucz 1995a,b for descriptions of these data), and altered the transition probabilities to provide acceptable matches to the spectrum of the similar metallicity giant HD 122563; see Eriksson et al. (1998) for a more complete description. Application of this line list to predict the HD 115444 spectrum yielded the synthetic spectra in the middle panel of Figure 6. We could deduce only an upper limit to the thorium abundances here:  $\log \epsilon(\text{Th}) \leq -2.2$ .

We tried to identify lines of uranium in the HD 115444 spectrum. Our brief reconnaissance produced only a potentially detectable U II feature at  $\lambda 3859.58 \text{ \AA}$ . Again, no absorption is obvious in the observed spectrum (bottom panel, Figure 6). Using the same procedure as we did for the Th II  $\lambda 4086 \text{ \AA}$  line, we created a line list for this spectral region and computed synthetic spectra for HD 115444. From the observed/synthetic spectrum comparison, we suggest that  $\log \epsilon(\text{U}) \leq -2.5$ .

We also obtained McDonald and Keck I spectra at very high S/N for the bright, very metal-poor giant HD 122563. This star, however, is deficient in neutron-capture elements ( $[\text{Eu}/\text{Fe}] \simeq -0.44$ ). We expected a weak-to-absent Th II  $\lambda 4019 \text{ \AA}$  line, and found none on the

observed spectrum. A synthetic spectrum computation yielded only that  $\log \epsilon(\text{Th}) \leq -3.1$ . A Keck spectrum was obtained for CS 22892-052, and although it has high resolution, the S/N is low. Therefore we chose to smooth this spectrum (sacrificing resolution for S/N) and then to merge it with the CTIO 4m echelle spectrum employed by Sneden et al. (1996). We again first derived  $^{12}\text{C}/^{13}\text{C} \simeq 16$  (in excellent agreement with the estimate of Norris et al. 1997) from other CH features in the CS 22892–052 spectrum. Then analysis of the  $\lambda 4019 \text{ \AA}$  blend suggested  $\log \epsilon(\text{Th}) = -1.60 \pm 0.1$  (Sneden et al. derived  $-1.55$  from just their CTIO spectrum).

A summary of our new abundance results for HD 115444, HD 122563, and CS 22892-052 is given in Table 1. We also used synthetic spectrum computations of the strong Eu II lines at  $\lambda\lambda 4129, 4205 \text{ \AA}$  to derive new values of the europium abundances in these stars. Our results here are in good accord with previous determinations (Griffin et al. 1982, Gilroy et al. 1982, Sneden et al. 1996, 1998). We have not obtained spectra of the radioactive elements in HD 126238, and thus this star will play no part in the age discussion to follow.

## 4.2. Ages

Thorium and uranium are produced solely in the *r*-process (presumably in a Type II supernova?). With the robust fits between stable stellar (and solar) abundances and the theoretical curves as discussed in §2 and §3, we may use the theory to predict the zero decay-age abundances of the radioactive elements thorium and uranium in the same calculation that reproduced the observed stable elements. We have therefore compared our theoretical estimates for the initial radioactive abundances with observed abundances in the metal-poor halo stars. Recall from Figure 1, where the abundances were compared before and after decay, that the calculations match very well (after decay) all the stable *r*-process nuclei (even the heaviest Pb and Bi isotopes) in the solar system. That agreement

strengthens our abundance predictions for the radioactive nuclei synthesized in the  $r$ -process.

The predicted Th/Eu ratio at zero decay-age based upon the least-squares-fit ETFSI-Q model is 0.426, or  $\log \epsilon(\text{Th}/\text{Eu})_0 = -0.37$ . We compared this value with the observed  $\log \epsilon(\text{Th}/\text{Eu})_*$  abundance ratios for the three very metal-poor halo stars given in Table 1. Using standard radioactive-age decay techniques (see e.g., Cowan et al. 1997) we find the following ages for HD 115444, CS 22892-052, and HD 122563 : 15.4, 10.7,  $> 6$  Gyr, respectively. Ignoring the case for HD 122563, where we only have an upper limit, we note that the Th/Eu ratio in the other two stars agree within observational uncertainties. Averaging the ratios for these two stars (i.e., using  $\log \epsilon (\text{Th}/\text{Eu}) = -0.65$ ), yields an average age for the very low metallicity stars of approximately 13.0 Gyr. Sneden et al. (1996) originally estimated an uncertainty in the  $\epsilon(\text{Th}/\text{Eu})$  of  $\pm 0.08$  for CS 22892-052, which yielded an age uncertainty of about  $\pm 3.7$  Gyr. The only error sources considered then were observational/analytical uncertainties in the abundance determination. With two stars analyzed here, yielding the nearly the same Th/Eu ratios, we estimate the uncertainties to be decreased slightly, and suggest an “observational” age uncertainty for the stellar pair to be  $\pm 3.5$  Gyr.

Although not as easily obtainable as in the case of the observations, we also determined a “theoretical” age uncertainty. We have employed the ETFSI-Q lsq. model in our calculations, and we have argued (§2) that it is the proper choice for the most reliable abundance determinations. For example, consider Eu and Th. The observed solar system elemental abundances by number are  $0.0907 \pm 0.0032$  and  $0.0420 \pm 0.0023$  respectively (on a scale where  $N(\text{Si}) = 10^6$ ). The ETFSI-Q predicted abundances for these two elements are 0.102 and 0.0433, which deviate by only roughly 10%. This 10% variation translates into an age uncertainty of approximately 2 Gyr, i.e.  $13 \pm 2$  Gyrs. We have also performed

numerical experiments to determine how sensitive the calculations are to applying this formula to solar system elemental and isotopic abundances. We altered the slope in the  $n_n$  distribution (superposition) of the ETFSI-Q curve to discover the maximum variation possible in the predicted Th abundance that would still be consistent with fitting this curve to the observed abundances of the major  $r$ -process peaks. The tail of this slope will influence the abundances of the heaviest elements (including Th) and is therefore the most relevant concern here. For the isotopic abundances in the range  $A=125\text{--}209$ , our numerical experiments yield an uncertainty characterized by a reduced  $\chi^2=0.76$ , which indicates that the predicted values are not significantly statistically different than the observed solar system values. If instead we compare predicted and observed *elemental* abundances in the range  $56\leq Z\leq 83$ , we find a reduced  $\chi^2=0.86$ , again reflecting good agreement and with deviations typically in the 10% range. Here we chose to adopt approximately twice that, or 20% error, as the most conservative measure of the theoretical uncertainty. This would suggest a Th age uncertainty of 3.7 Gyr, comparable to the value found for the observations. Adding in quadrature the observational age uncertainty (as discussed above) to this uncorrelated theoretical uncertainty yields a total age uncertainty of approximately 5 Gyr. The estimated age of 13.0 Gyr remains virtually unchanged from our previous estimates (Cowan et al. 1997, Pfeiffer et al. 1997).

The uranium abundance in HD 115444 is a very weak upper limit, and in fact the value may be much lower. Nevertheless, we can make some age estimate based upon this upper limit. We note, however, that unlike the Th elemental abundance which depends only upon one isotope, the uranium abundance results from the decay of two radioactive isotopes with very different half-lives. In the ETFSI-Q model the initial elemental abundance is dominated by the shorter half-life isotope,  $^{235}\text{U}$ , while presumably the elemental abundance in the metal-poor stars is mostly determined by  $^{238}\text{U}$ . Ignoring the initial  $^{235}\text{U}$  production entirely (this isotope decays in much less than a Hubble time), and only comparing the

initial time-zero  $^{238}\text{U}$  and the observed upper limit in HD 115444 gives a lower limit on the age of this star of  $> 7.1$  Gyr. While this age estimate has much observational and theoretical uncertainty, it is entirely consistent with the value found using the Th abundance.

## 5. Discussion and Conclusions

The abundance comparisons shown in the figures indicate several striking results. First, as noted already by Sneden et al. (1998), for the four metal-poor stars for which extensive data have become available, the stellar data are in solar  $r$ -process proportions (at least for  $Z \geq 56$ ). While this has been suggested now for a number of years, this trend is now seen over a wider elemental range, including data from the 3rd  $r$ -process peak, than was previously attainable. In this paper we have emphasized the use of theoretical  $r$ -process calculations, rather than observed solar system data, to confirm this trend. Furthermore, the fact that all four stars, covering a wide range of metallicities ( $[\text{Fe}/\text{H}] = -3.1$  to  $-1.7$ ), show the same consistent scaled solar  $r$ -process pattern make other explanations (such as a random superposition of abundances, see e.g., Goriely & Arnould 1997) much less likely. For elements with  $Z \geq 56$ , the relative elemental  $r$ -process abundances appear not to have changed over the history of the Galaxy. This further suggests that there is one  $r$ -process site in the Galaxy, at least for those elements.

However, the trend for the lighter neutron-capture elements with  $A < 100$  is not as clear, but may be explainable in terms of the emergence of the weak  $s$ -process with increasing metallicity. The abundance values of Zr and Ge, for example, are approximately the same in HD 115444 and HD 122563, two stars of the same metallicity but which show large differences in the absolute levels of heavy neutron-capture elements. The weak  $s$ -process is expected to be metallicity dependent as a secondary process, but to occur earlier than the main  $s$ -process component, as it is produced in (core He-burning of) massive stars

rather than (He-shell flashes of) low/intermediate mass stars. We note, however, that it is unclear how effective the weak  $s$ -process might be in stars of extremely low metallicity, and other explanations may be possible. One such possibility may be that there are two  $r$ -process signatures – one for the lighter and one for the heavier  $r$ -process nuclei – reflecting two separate sites (Wasserburg, Busso, & Gallino 1996; Qian, Vogel, & Wasserburg 1998). (See Wheeler, Cowan, & Hillebrandt 1998, and Freiburghaus et al. 1998 for a discussion of possible second sites.) It is also conceivable that this region of Sr-Zr could be produced by a combination of the  $r$ - and the weak  $s$ -process, as suggested for the star CS 22892–052 by Cowan et al. (1995). Clearly more observational and theoretical work will be required to understand the production of these lighter n-capture elements early in the history of the Galaxy.

The detection of thorium in very metal-poor stars (pioneered by François, Spite, & Spite 1993) has provided the exciting opportunity of directly determining stellar ages (see Sneden et al. 1996, Cowan et al. 1997 and Pfeiffer et al. 1997). In this paper we have used the stable stellar and solar data to constrain the predicted (zero decay-age) values of the radioactive  $r$ -process  $\emptyset$  nuclei. With detailed Th II analyses now in two very metal-poor stars, we have extended our previous age determinations to give an average age estimate of about 13.0 Gyr for very old halo stars, supporting previous age estimates for CS 22892–052 from Cowan et al. (1997) and Pfeiffer et al. (1997). It is encouraging to note that our new age estimate for these two stars is consistent with recent globular cluster age determinations based upon Hipparcos data (see Pont et al. 1998). We also note the consistency of this age estimate with the recent cosmological age estimate of  $14 \pm 1.5$  Gyr (Riess et al. 1998). We caution, however, that there are still several uncertainties which limit the accuracy of these radioactive age determinations. In particular, small changes in the abundance determinations can result in large age uncertainties due to the exponential decay-time dependence. The resulting age similarities for the two stars for which data are available,

however, do lend support to using this technique, which we emphasize is independent of chemical evolution models. To refine further and strengthen this technique will require many more observations of the long-lived radioactive elements in other metal-poor halo stars. Additional theoretical calculations, employing full, dynamic  $r$ -process calculations, suitable for astrophysical environments, will also be needed to make more accurate stellar and Galactic age determinations.

We thank John Norris and Jim Lawler for helpful conversations, and appreciate the expert help of the STScI staff in all aspects of the planning and execution of the observations over three HST Cycles. We thank Dr. Barbara Neas and Dr. L. D. Cowan, Dept. of Biostatistics and Epidemiology at OUHSC, for helpful advice on statistics and uncertainties. Support for this work was provided through grants GO-05421, GO-05856, and GO-06748 from the Space Science Telescope Institute, which is operated by the Association of Universities for Research in Astronomy, Inc., under NASA contract NAS5-26555. Support was also provided by the National Science Foundation (AST-9314936 and AST-9618332 to J.J.C.), (AST-9315068 and AST-9618364 to C.S.) and (AST-9529454 to T.C.B.), by the Swiss Nationalfonds (grants 20-47252.96 and 2000-53798.98), and by the German BMBF (grant 06Mz864) and DFG (grant Kr8065). J.J.C. and F.-K.T. thank the Institute for Theoretical Physics at the University of California at Santa Barbara, for partial support from the National Science Foundation under Grant No. PHY94-07194. This work was completed while J.J.C. was in residence at the University of Texas at Austin, funded through the University of Oklahoma as a Big XII Faculty Fellow; we are very grateful to both institutions for their support of this research.

## REFERENCES

- Aboussir, Y., Pearson, J. M., Dutta, A. K., & Tondeur, F. 1995, *At. Data Nucl. Data Tables*, 61, 127
- Anders, E., & Ebihara, M. 1982, *Geochim. Cosmochim. Acta*, 46, 2363
- Anders, E., & Grevesse, N. 1989, *Geochim. Cosmochim. Acta*, 53, 197
- Burris, D. L., Pilachowski, C. A., Armandroff, T., Sneden, C., & Cowan, J. J. 1998, in preparation
- Chen, B., Dobaczewski, J., Kratz, K.-L., Langanke, K., Pfeiffer, B., Thielemann, F.-K., & Vogel, P. 1995, *Phys. Lett.*, B355, 37
- Cowan, J. J., Burris, D. L., Sneden, C., McWilliam, A., & Preston, G. W. 1995, *ApJ*, 439, L51
- Cowan, J.J., Sneden, C., Truran, J. W., & Burris, D. L. 1996, *ApJ*, 460, L115
- Cowan, J.J., Thielemann, F.-K., & Truran, J.W. 1991, *Phys. Rep.*, 208, 267
- Cowan, J.J., McWilliam, A., Sneden, C., & Burris, D. L. 1997, *ApJ*, 480, 246
- Eriksson, K., Edvardsson, B., Sneden, C., Burles, S., & Tytler, D. 1998, in preparation
- François, P. & Gacquer, W. 1998, *Nature*, submitted
- François, P., Spite, M., & Spite, F. 1993, *A&A*, 274, 821
- Freiburghaus, C., Rembgas, J.-F., Rauscher, T., Thielemann, F.-K., Kratz, K.-L., Pfeiffer, B., & Cowan, J. J. 1998, *ApJ*, in press
- Gilroy, K. K., Sneden, C., Pilachowski, C. A., & Cowan, J. J. 1988, *ApJ*, 327, 298

- Goriely, S., & Arnould, M. 1996, *A&A*, 312, 327
- Goriely, S., & Arnould, M. 1997, *A&A*, 322, L29
- Gratton, R., & Sneden, C. 1991, *A&A*, 241, 501
- Gratton, R., & Sneden, C. 1994, *A&A*, 287, 927
- Griffin, R., Griffin, R., Gustafsson, B., & Vieira, T. 1982, *MNRAS*, 198, 637
- Hoff, R. 1986, in *Weak and Electromagnetic Interactions in Nuclei*, ed. H.V. Klapdor (Heidelberg: Springer), 207
- Hoff, R. 1987, *J. Phys. G.*, 24, S343
- Käppeler, F., Beer, H., & Wisshak, K. 1989, *Rep. Prog. Phys.*, 52, 945
- [Käppeler, F. 1998, in *Nuclei in the Cosmos V*, in press]
- Kratz, K.-L., Thielemann, F.-K., Hillebrandt, W., Möller, P., Harms, V., & Truran, J. W. 1988, *J. Phys. G*, 14, 331
- Kratz, K.-L., Bitouzet, J.-P., Thielemann, F.-K., Möller, P., & Pfeiffer, B. 1993, *ApJ*, 403, 216
- Kratz, K.-L. 1998, in *Proc. 2nd Int. Conf. on Exotic Nuclei and Atomic Masses -ENAM98*, in press
- Kurucz, R. L. 1995a, in *Astrophysical Applications of Powerful New Databases*, *PASP Conf. Ser.* 78, eds Adelman, S. J. & Wiese, W. L. (San Francisco, ASP), 205
- Kurucz, R. L. 1995b, in *Laboratory and Astronomical High Resolution Spectra*, *PASP Conf. Ser.* 81, eds Sauval, A. J., Blomme, R., & Grevesse, N., (San Francisco, ASP), 583

- Magain, P. 1995, *A&A*, 297, 686
- Mathews, G. J., Bazan, G., & Cowan, J. J. 1992, *ApJ*, 391, 719
- McWilliam, A. 1997, *ARAA*, 35, 503
- McWilliam, A. 1998, *AJ*, in press
- McWilliam, A., Preston, G. W., Sneden, C., & Searle, L. 1995a, *AJ*, 109, 2736.
- McWilliam, A., Preston, G. W., Sneden, C., & Searle, L. 1995b, *AJ*, 109, 2757.
- Meyer, B. S. 1994, *ARA&A*, 32, 153
- Möller, P., Nix, J.R., Myers, W.D., & Swiatecki, W.J. 1995, *At. Data Nucl. Data Tables* 59, 185
- Möller, P., Nix, J.R., & Kratz, K.-L. 1997, *At. Data Nucl. Data Tables* 66, 131
- Möller, P., & Randrup, J. 1990, *Nucl. Phys.* A514, 1
- Morell, O., Källander, D., & Butcher, H. R. 1992, *A&A*, 259, 543
- Norris, J. E., Ryan, S. G., & Beers, T. C. 1997, *ApJ*, 490, L169
- Pearson, J. M., Nayak, R. C., & Goriely, S. 1996, *Phys. Lett.* B387, 455
- Pfeiffer, B., Kratz, K.-L., & Thielemann, F.-K. 1997, *Z. Phys.* A, 357, 235
- Pilachowski, C. A., Sneden, C., & Kraft, R. P. 1996, *AJ*, 111, 1689
- Pont, F., Mayor, M., Turon, C., & Vandenberg, D. A. 1998, *A&A*, 329, 87
- Qian, Y.-Z., Vogel, P., & Wasserburg, G. J. 1998, *ApJ*, 494, 285
- Qian, Y.-Z., & Woosley, S. E. 1996, *ApJ*, 471, 331

- Riess, A. et al. 1998, AJ, submitted
- Sneden, C. 1973, ApJ, 184, 839
- Sneden, C., & Parthasarathy, M. 1983, ApJ, 267, 757
- Sneden, C., & Pilachowski, C.A. 1985, ApJ, 288, L55
- Sneden, C., Preston, G. W., McWilliam, A., & Searle, L. 1994, ApJ, 431, L27
- Sneden, C., McWilliam, A., Preston, G. W., Cowan, J. J., Burris, D. L., & Armosky, B. J.  
1996, ApJ, 467, 819
- Sneden, C., Cowan, J. J., Burris, D. L., & Truran, J. W. 1998, ApJ, 496 in press
- Spite, M., & Spite, F. 1978, A&A, 67, 23
- Takahashi, K., Witt, J., & Janka, H.-T. 1994, A&A, 286, 857
- Thielemann, F.-K., Kratz, K.-L., Pfeiffer, B., Rauscher, T., van Wormer, L., & Wiescher,  
M. 1994, Nucl. Phys. A, 570, 329c
- Thielemann, F.-K., Freiburghaus, C., Kolbe, E., Rauscher, T., Rembges, F., Kratz, K.-L.,  
Pfeiffer, B., Schatz, H., Wiescher, M., & Cowan, J.J. 1998, in Proceedings of the 9th  
Capture Gamma-Ray Spectroscopy Symposium, ed. G. Molnar, (Budapest: Springer  
Hungarica) in press
- Truran, J. W. 1981, A&A, 97, 391
- Tull, R. G., MacQueen, P. J., Sneden, C., and Lambert, D. L. 1995, PASP, 107, 251
- Vogt, S. S. 1992, in ESO Workshop on High Resolution Spectroscopy with the VLT, ed. M.  
H. Ulrich (ESO, Garching), p. 223
- Wasserburg, G.J., Busso, M., & Gallino, R. 1996, ApJ, 466, L109

Wheeler, C., Cowan, J. J., & Hillebrandt, W. 1998, ApJ, 493, L101

Wisshak, K., Voss, F., & Käppeler, F. 1996, in Proceedings of the 8<sup>th</sup> Workshop on Nuclear Astrophysics, ed. W. Hillebrandt, & E. Müller (Munich: MPI), 16

Woosley, S. E., Wilson, J. R., Mathews, G. J., Hoffman, R. D., & Meyer, B. S. 1994, ApJ, 433, 229

Table 1. Neutron-Capture Element Abundances

Transition	log $\epsilon$ HD 115444	log $\epsilon$ CS 22892-052	log $\epsilon$ HD 122563
Derived Abundances			
Th II $\lambda 4019 \text{ \AA}$	-2.10	-1.6	<-3.1
Th II $\lambda 4086 \text{ \AA}$	<-2.2	...	...
U II $\lambda 3860 \text{ \AA}$	<-2.5	...	...
Eu II $\lambda \lambda 4129, 4205 \text{ \AA}$	-1.55	-0.89	-2.58
Abundance Ratios			
Th/Eu	-0.6	-0.7	<-0.5
U/Eu	<-1.0	...	...
Th/U	>+0.4	...	...

### Figure Captions:

Fig. 1.— Comparison of theoretical abundances with solar  $r$ -process abundances (small filled circles). The dashed line indicates abundances prior to beta- and alpha-decay and the solid line the final abundances after decay. The crosses represent calculated abundances after decay for the nuclei  $^{232}\text{Th}$ ,  $^{235}\text{U}$ ,  $^{238}\text{U}$  and  $^{244}\text{Pu}$  in comparison with the solar values (filled circles) for these nuclei. (See text for discussion.)

Fig. 2.— Comparison of observed abundances (large filled squares) from CS 22892-052 and solar  $r$ -process abundances (small filled circles) joined by a dashed line with a theoretical  $r$ -process abundance distribution denoted by a solid line. (See text for discussion.)

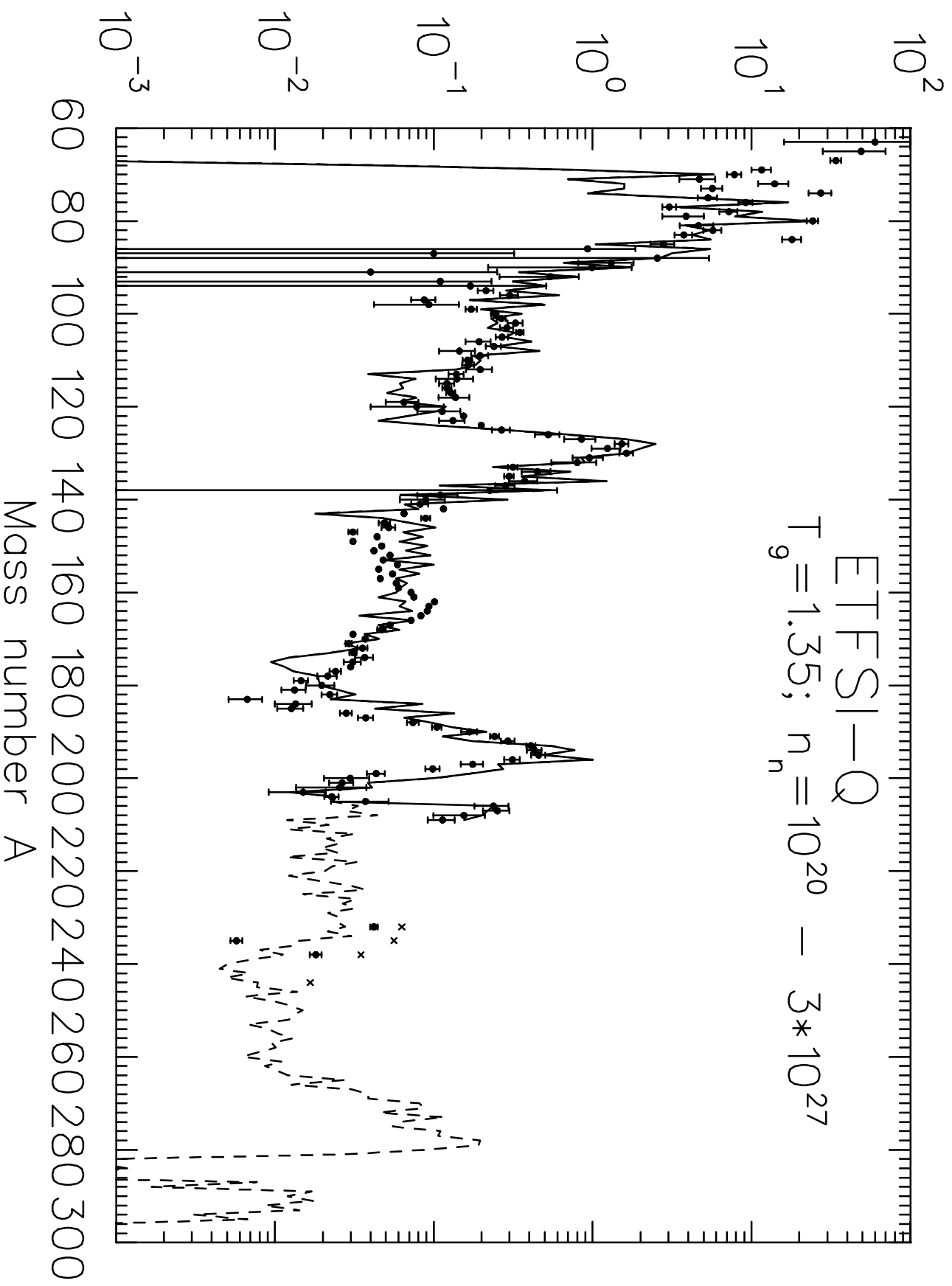
Fig. 3.— An abundance comparison between the neutron-capture elements in HD 115444 and a theoretical  $r$ -process (solid line) and a solar system  $r$ -process (dashed line) abundance distribution. Ground-based data (from various sources, see text for discussion) are indicated by open squares, while HST data from Sneden et al. (1998) are indicated by solid squares.

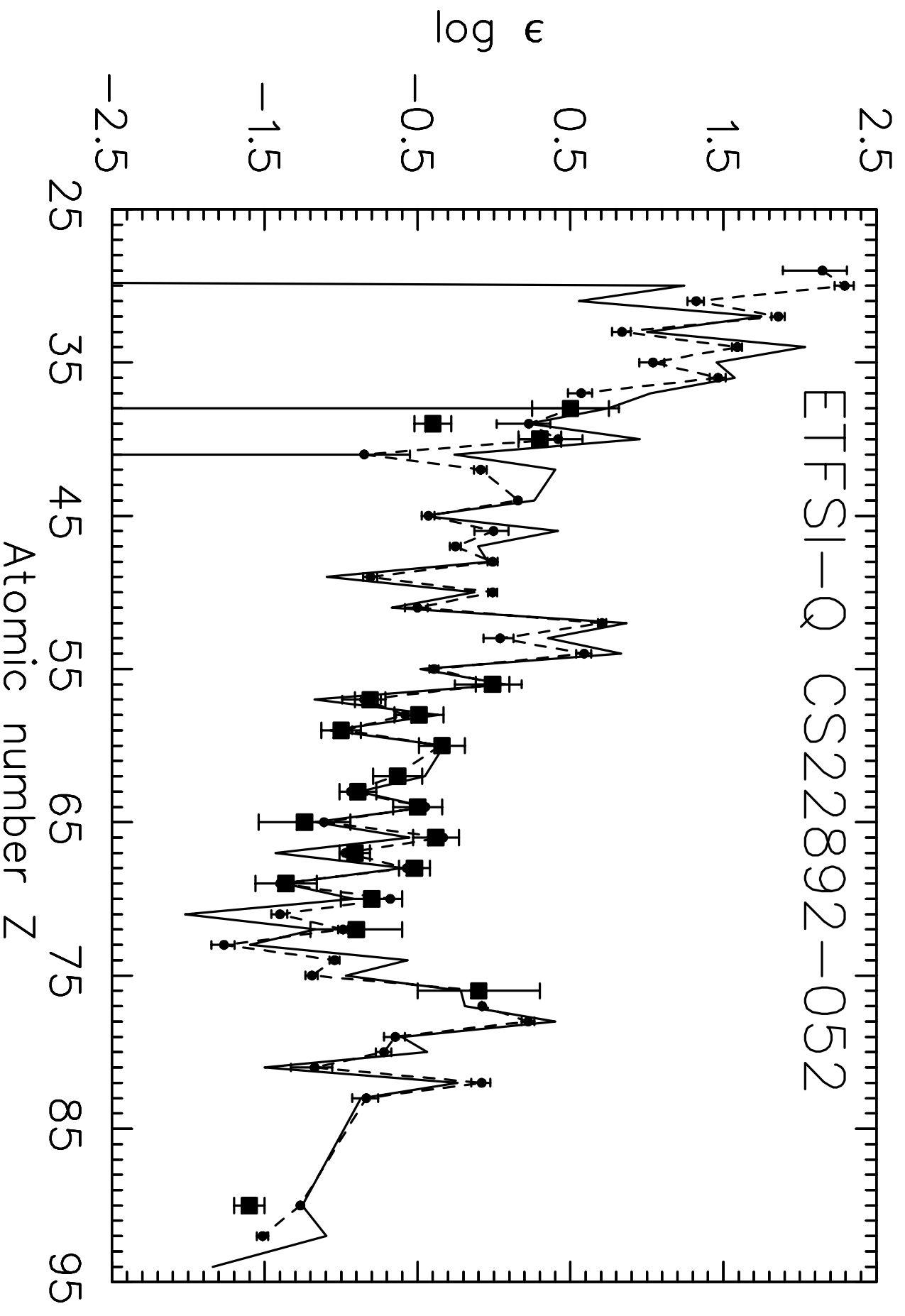
Fig. 4.— An abundance comparison for HD 122563 in the same style as that of Figure 3. Upper limits for Os and Pt are indicated by crosses with attached arrows.

Fig. 5.— An abundance comparison for HD 126238 in the same style as that of Figure 3.

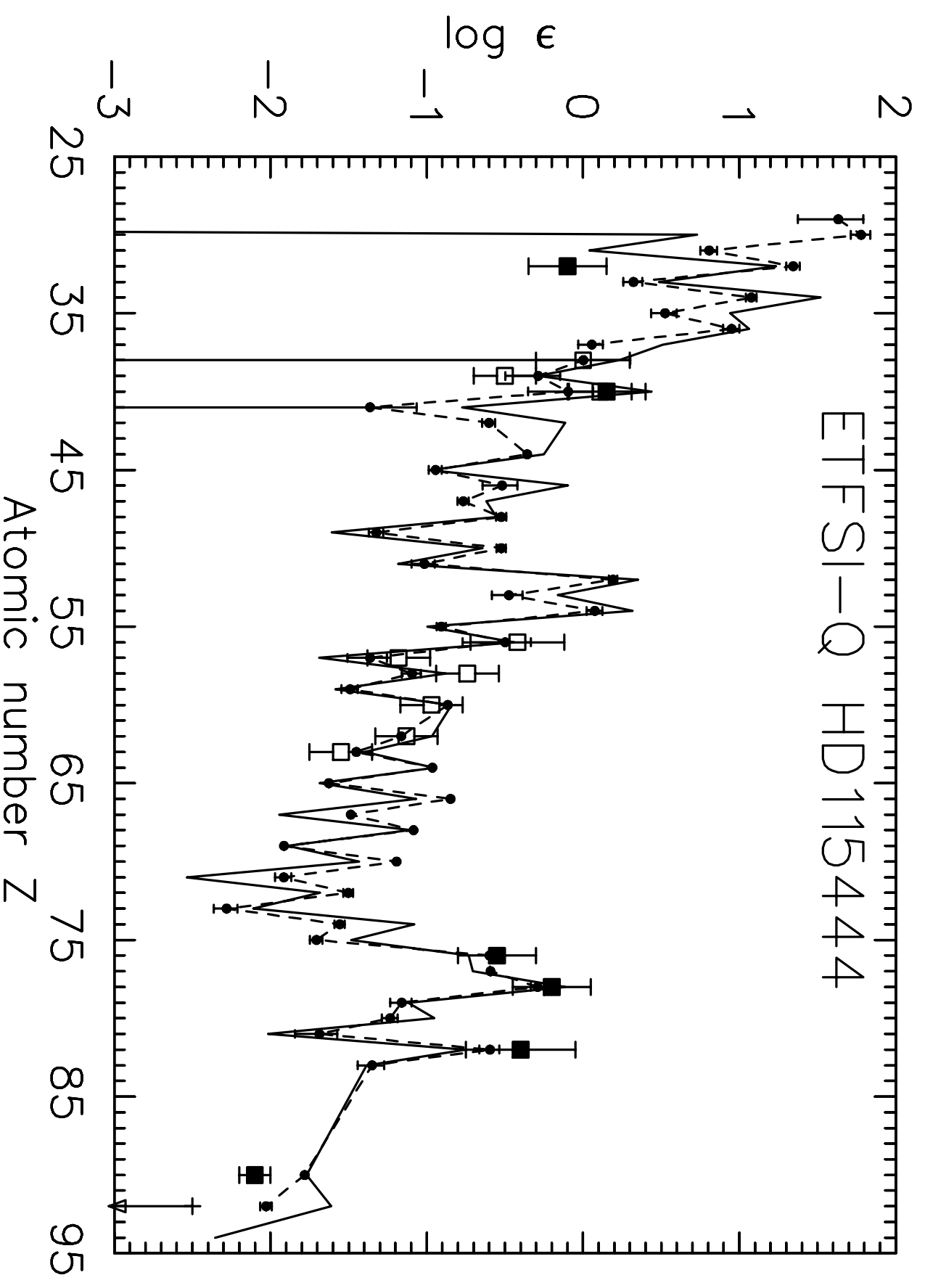
Fig. 6.— Observed and synthetic spectra of thorium and uranium transitions in the spectrum of HD 115444. See text for discussion of the observational data and the synthetic spectrum computations.

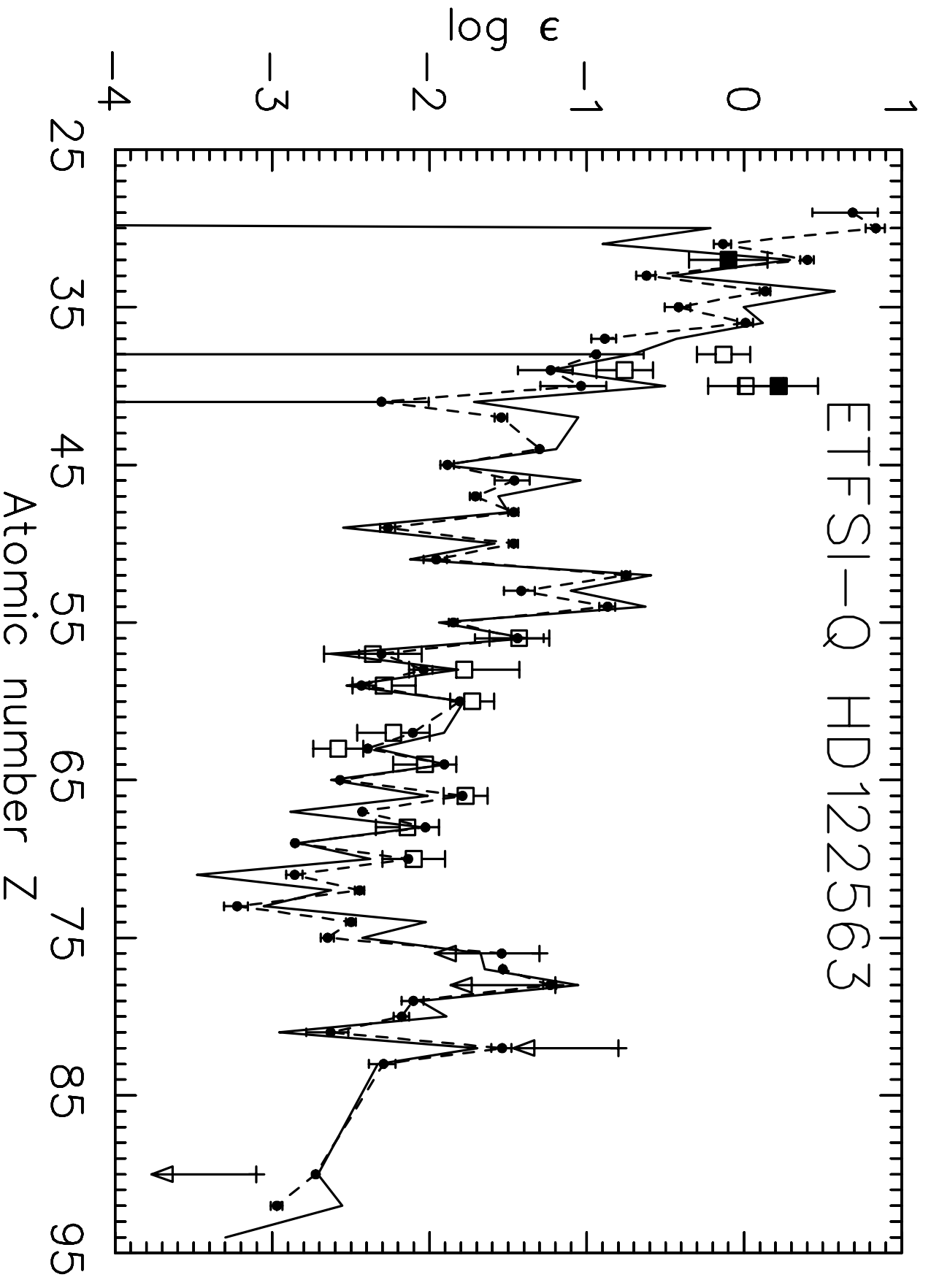
Solar r-abundance





ETFSl-Q HD115444





ETFSI-Q HD126238

